Microchemical Journal 200 (2024) 110303

Contents lists available at ScienceDirect

Microchemical Journal

journal homepage: www.elsevier.com/locate/microc

Cu(II)-binder complexes in azurite and malachite pictorial mixtures: An EPR study

Riccardo Punis [a,*], Alfonso Zoleo [a,b]

[a] DiSC, Dipartimento di Scienze Chimiche, Università degli Studi di Padova, Via Marzolo, 1, 35131 Padova
[b] CIBA, Center for Research, Study and Conservation of Archaeological, Architectural and Historical-Artistic Heritage, CIBA, University of Padova, 2-35122 Padova, Italy

ARTICLE INFO

Keywords:
Malachite
Azurite
Copper
CW-EPR
Metal soaps
Pictorial mixtures

ABSTRACT

Degradation processes of paintings, frescos, illuminations, and painted decorations represent a relevant challenge in the cultural heritage field for both conservators and scientists dealing with the causes of these processes. It is very important understanding the molecular origin of colour changes, like fading, yellowing, blackening, as well as the molecular origin of damages due to degradation, like cracking and fall of pictorial layers. Metal complexes, often indicated as "metal soaps", when referred to metal carboxylates, play a relevant role in degradation. However, their identification is not easy, and the involvement of the metal ions in the degradation mechanisms is often not clear. Continuous Wave Electron Paramagnetic Resonance (CW-EPR) spectroscopy is a very sensitive tool towards paramagnetic species (e.g., transition metal ions like Fe(III), Cu(II), Mn(II), radicals, etc.), providing relevant information on these species, not always well-characterized with other methods. In this paper, we use CW-EPR to study the formation of Cu(II)-binder complexes in natural malachite and azurite pigments mixed with several organic binders. We show that CW-EPR technique is able to detect easily Cu(II) complexes with organic ligands, and can additionally provide information on the pigments themselves. In particular, the first coordination sphere of the Cu(II) complexes is characterized by applying the Peisach-Blumberg method. Moreover, CW-EPR shows that binders can affect the structure of the raw pigments.

1. Introduction

The art of making pigments, treating them, creating mixtures, and the techniques for painting, remained orally handed down for many centuries. Around the end of the 14th century and the beginning of the 15th, Cennino Cennini decided to report this information into a monographic manuscript [1], allowing us to have a hint on the manufacture processes exploited by artists in the ancient centuries. One of the most relevant pieces of knowledge reported in "The Book of Art" concerns the materials used to produce artifacts, the inorganic pigments, and their production methods. Natural pigments were usually excavated from readily available sources like rocks, clays, etc [1]. Then, the selected material was simply ground, washed, and sieved. Among the natural inorganic pigments, azurite ($Cu_3(OH)_2(CO_3)_2$) and malachite ($Cu_2CO_3(OH)_2$) are copper-based inorganic pigments widely used for their nice blue and green tones, respectively. Malachite was probably the oldest known green pigment, and it is abundant all over the world [2]. Large ore deposits are present in the Ural Mountains and Hungary and probably the one in Hungary was the main ore deposit in medieval times. Even some Chinese and Japanese pieces of art were colored with malachite. Cennini reports that malachite can be also artificially produced from another similar pigment: azurite [1].Azurite is commonly found in the malachite ores, as they are chemically similar. This pigment was for many centuries the most important light blue pigment, together with lapis lazuli. In fact, very often suppliers passed off azurite as ultramarine blue, which was a more expensive pigment. Malachite and azurite share the same chemical nature, but the crystal structure is quite different [3,4]. In particular, in the azurite structure the Cu^{2+} cations are placed in two sites, one with square planar arrangement and the other with square pyramidal environment. In the malachite structure, the copper atoms are located into two slightly distorted octahedral sites. When azurite is exposed to air and humidity, conversion of azurite into malachite is a possible process, according to the following reaction [3,4]:

$$2\left[2CuCO_3{\cdot}Cu(OH)_2\right] + H_2O \rightarrow 3\left[CuCO_3{\cdot}Cu(OH)_2\right] + CO_2$$

* Corresponding author.
E-mail address: riccardo.punis@phd.unipd.it (R. Punis).

https://doi.org/10.1016/j.microc.2024.110303
Received 28 January 2024; Received in revised form 6 March 2024; Accepted 7 March 2024
Available online 12 March 2024
0026-265X/© 2024 The Author(s). Published by Elsevier B.V. This is an open access article under the CC BY-NC-ND license (http://creativecommons.org/licenses/by-nc-nd/4.0/).

e conversion becomes apparent thanks to the color change from blue to green, typical of malachite pigment. However, when azurite is combined with *tempera* and oil it is quite stable and does not turn into malachite [3,4], but both azurite and malachite can change their color and optical properties when combined with organic binders [5]. This is due to the coordination change of Cu^{2+} cations. It has been shown that linseed oil is able to "extract" the copper ions from the inorganic moiety of the mixture and create new complexes with different optical properties, leading to a color change in the pictorial mixture [5]. These complexes are often indicated with the generic term of "copper soaps". Among the spectroscopic tools useful to characterize copper complexes, Electron Paramagnetic Resonance spectroscopy (EPR) has recently emerged as a powerful and versatile technique [6–9]. EPR spectroscopy is a non-destructive technique capable of detecting paramagnetic species (at least one unpaired electron) such as organic radicals, electronic defects in solids and transition metals (e.g., Fe(III), Mn(II) and Cu(II)) [10,11]. EPR has been applied in the field of the cultural heritage for many years [12–14], but only in the last ten years an increasing interest in applying this technique to study pigment-ligand interactions has emerged [8,9,15].

In this study, we use CW-EPR to investigate the interaction between azurite and malachite pigments with several organic binders, selected for their relevance in the field of art, i.e., linseed oil, egg tempera (egg white and yolk), Arabic gum, and rabbit glue (collagen).

2. Research aim

In this study, the interaction of malachite and azurite with several organic binders has been studied through Continuous Wave - Electron Paramagnetic Resonance (CW-EPR) spectroscopy. The binders were the ones commonly used in ancient times, i.e., linseed oil, Arabic gum, egg tempera (yolk and white), and rabbit glue. Main purpose of the work is the detection and characterization through CW-EPR of the Cu(II)-binder complexes produced in the pigment-binder mixtures. On the raw natural pigments, a crossed CW-EPR and XRF investigation allowed the detection and identification of minor paramagnetic species and superparamagnetic species. On one side, these species could be potentially useful to distinguish malachite and azurite from different natural ores, on the other, these "impurities" could play a role in degradation patterns.

3. Materials and methods

Several types of mixtures were prepared by mixing the pigments and the binder with two different pigment mass percentages for each selected binder. Each mixture is labelled P*nr*, where P, the pigment, is ML (malachite) or AZ (azurite), while *n*, the binder, is EW (egg white), Y (yolk), AG (Arabic gum), EY (egg white and yolk), LO (linseed oil), or C ("collagen", from rabbit glue), and *r*, the weight ratio, takes the value 75 (75 % w/w pigment mass percentage) and 5 (5 % w/w pigment mass percentage). E.g., MLEW75 indicates the mixture malachite and egg white, with a 75 % pigment in the mixture. Before the binders were mixed with the pigments, they were differently prepared. The Arabic gum was supplied by Winsor&Newton and no further treatments were done. Chicken eggs were used to obtain the different egg *temperas*. The egg white was separated from the yolk and filtered with filter paper until the density was optimal according to Cennino Cennini's traditional recipe (Cennini XIV-XV century). Since the yolk is protected by a phospholipid membrane, the latter was removed piercing it and the yolk was squeezed out. A few drops of ethanol were added to the egg white and to the yolk to avoid molding, getting the final binders EW and Y. To obtain the EY binder, the EW and Y moieties were simply mixed after their preparation. The rabbit glue was provided by Zecchi as rigid tablets. They were broken into small pieces and then completely immersed in water for 48 h. After this procedure, the glue absorbed the water and swelled. Then, it was heated for about 30 min at 60 °C, getting the final binder C, a slightly opalescent solution. Finally, the linseed oil, supplied by Zecchi, was exposed to light for at least a day, according to Cennini's recipe. The pigments were firstly ground in an agate mortar, and then mixed with the binders. Mixtures were spread on a piece of filter paper and dried at room temperature for at least 5 days. For the Y*n*75 samples, the dried films were scraped obtaining powders. These powders were analyzed by CW-EPR. For the Y*n*5 samples, it was not possible to scrape the dried films. Therefore, a piece of the filter paper on which the mixture was spread and dried was cut and analyzed by EPR spectroscopy (the paper alone did not show any EPR signal). The CW-EPR measurements of the mixtures were performed at room temperature, 250, 210, 180 and 150 K with a Bruker ECS 106 spectrometer equipped with a Bruker resonator 4108 TMH at X-Band (~9.5 GHz) and an external nitrogen-based cooling system. A 100 KHz modulation of the magnetic field was applied for the continuous wave experiments. The CW spectra were simulated with the software Easy Spin [16]. XRF experiments were performed with a Bruker ARTAX^{TM} 200. A Coolidge X-Ray tube with Mo anode was used. Voltage was set to 45 kV and tube current 0.705 mA, with 3 min. scan for each measurement.

4. Results and discussion

4.1. CW-EPR: Raw pigments (ML and AZ)

The CW-EPR spectrum at room temperature of ML sample is displayed in Fig. 1. The assignation of the signals is complicated, and the spectrum appears quite crowded. However, some of the main features could be assigned. The two signals marked with the blue asterisks, centered at 80 mT a and at 166 mT respectively, could be related to the presence of either Fe(III) or Mn(II) species [17]. However, the XRF spectrum of the ML sample does not show any manganese-related signal (Figure S1). Only a very low-intense peak of Fe appears. Therefore, those signals are likely assignable to Fe(III) species. The signal centered at 340 mT could be related to both Cu(II) and Fe(III) species. Probably, the signal arises from the superimposition of the two EPR-active species. The wiggles at 380 mT indicate this superimposition. In the spectral region between 180 and 330 mT, many interesting features are present in the spectrum. These are probably due to the presence of superparamagnetic species e.g., very small particles of iron oxide, copper oxide, etc [18,19]. The superparamagnetic behavior of some compounds comes from the coupling of several paramagnetic species. These coupling mixes the spins state of the species, generating new spin states with higher or lower spin numbers depending on the nature of the coupling (i.e., antiferromagnetic or ferromagnetic). When the ferromagnetic systems are smaller than a single Weiss domain, a "superparamagnetic" behavior emerges. It is reported in literature that the line width, the shape, and the resonance field (g-factor) of the EPR signal of superparamagnetic species change strongly with the temperature [18,19]. In order to establish if the EPR signals in ML were related to superparamagnetic species, we collected the EPR spectra of ML at different temperatures, i.e., 250 K, 210 K, 180 K and 150 K. What emerges from the temperature scanning is that the signals change their shape, line width and resonant field, in agreement with the hypothesis of superparamagnetic species. However, it is very difficult following the evolution with temperature of each signal because of spectral crowdedness (Fig. 2).

Similarly, the azurite shows features like those found for malachite (Fig. 3 and Figure S2). However, the nature of the superparamagnetic species seems to be different according to position, intensity and shape of the peaks (Figure S3). The temperature-sweep for raw azurite is displayed in Figure S4. In this context, it is even more challenging to attempt an assignment to specific compounds for the features. According to the crystal structure of malachite and azurite, it could be possible that copper atoms, inside the pigment crystal structure, couple magnetically to each other [20,21]. However, in order to achieve a superparamagnetic arrangement, another mandatory condition must be

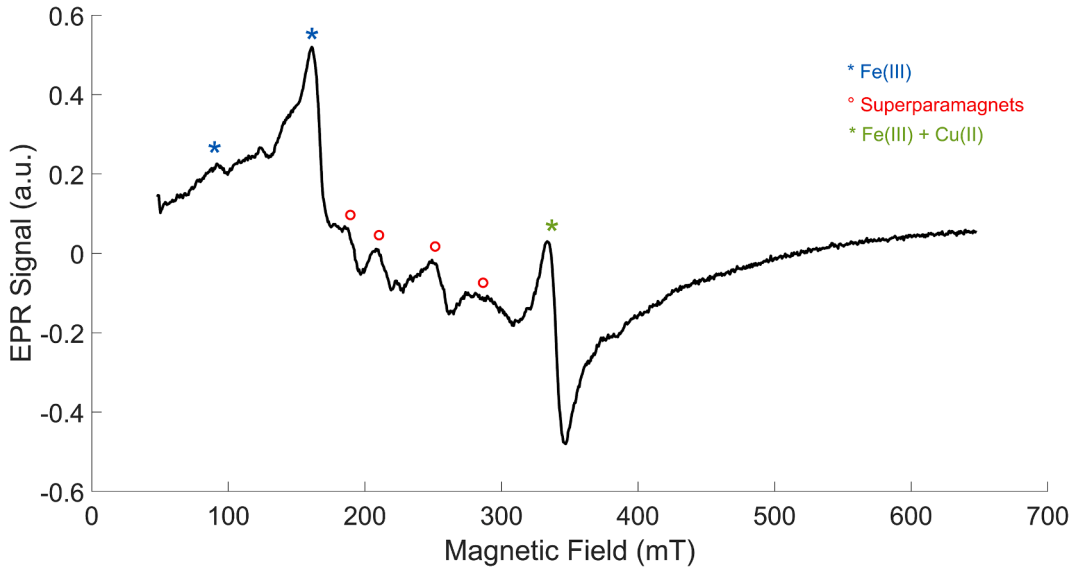

Fig. 1. Raw malachite (ML) CW-EPR spectrum at X-band collected at room temperature. The blue asterisks indicate the Fe(III) signals, while the red circles are related to superparamagnetic species signals (e.g. copper oxide, iron oxides, etc.). (For interpretation of the references to color in this figure legend, the reader is referred to the web version of this article.)

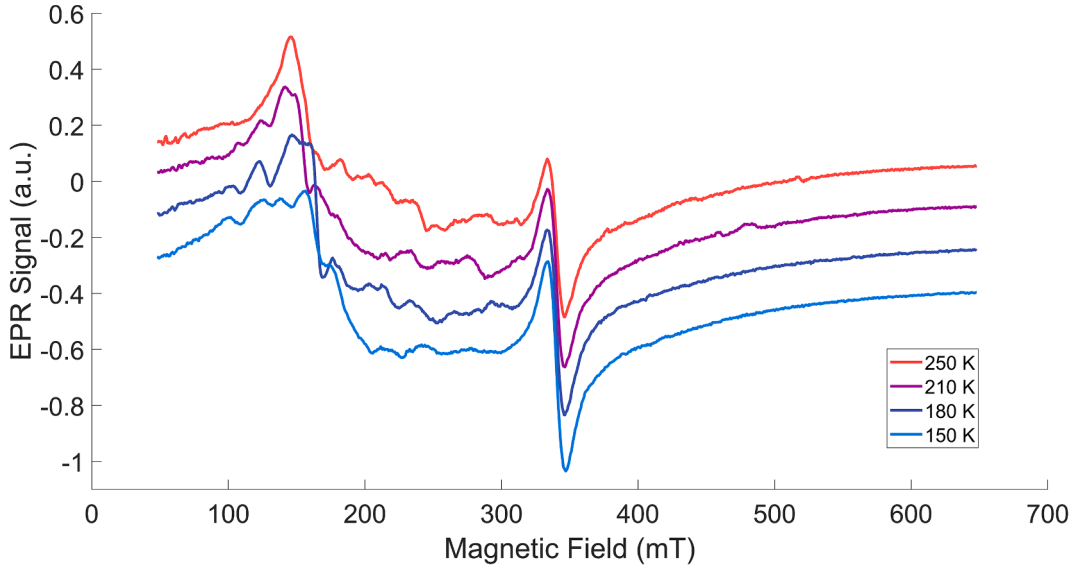

Fig. 2. Raw malachite (ML) CW-EPR spectra at X-band collected at 250 K (red line), 210 K (purple line), 180 K (dark blue line) and 150 K (light blue line). (For interpretation of the references to color in this figure legend, the reader is referred to the web version of this article.)

fulfilled: the pigment particles must have very fine size (i.e. 3–50 nm) [22]. As shown by CW-EPR spectra, both of the two conditions were achieved in the raw pigments.

4.2. CW-EPR: MLnr pictorial mixtures

The EPR spectra of the MLn75 mixtures are displayed in Figure S5. It is evident that the spectra of the mixtures are always different than the pure pigment, indicating that the binders generate new coordination compounds with the paramagnetic species present in the pigment. It can be noticed that the signal at 330 mT becomes slightly broader than in the spectrum of raw malachite. This could suggest, also considering the modification of the other spectral features (e.g., the signal at 150 mT and the superparamagnetic features), that the binder can change the coordination of Fe^{3+} cations, present in the pigment as natural impurities. A clear emerging of features related to Cu(II)-binder complexes cannot be seen. For this reason, we analyzed samples with a higher relative quantity of binders. In Figure S6, the EPR spectra of MLn5 mixtures are shown: for MLAG5, MLY5, MLEY5 the pattern of a paramagnetic Cu(II) complex is observed. The pattern is characterized by a single strong line at about 330 mT (due to the x and y component of the g-tensor) and a quartet of lines at lower field (component z of the g-tensor). The distance between two close lines of the quartet is the hyperfine constant A_{zz} (component z of the hyperfine tensor), which is strongly dependent on the type of Cu(II) complex [6]. Two main aspects can be noticed. Firstly, it seems that the arabic gum (MLAG5), the yolk (MLY5), the egg tempera (MLEY5) are the most suitable binders to form specific copper complexes. Collagen (MLC5) seems to be efficient in generating copper complexes, but the absence of a clear quartet pattern at low field suggests that many different types of complexes are formed (non-specific binding), overlapping such a way to cancel out the quartet pattern. On the other hand, in the MLLO5 spectrum signals due to Cu(II)-binder

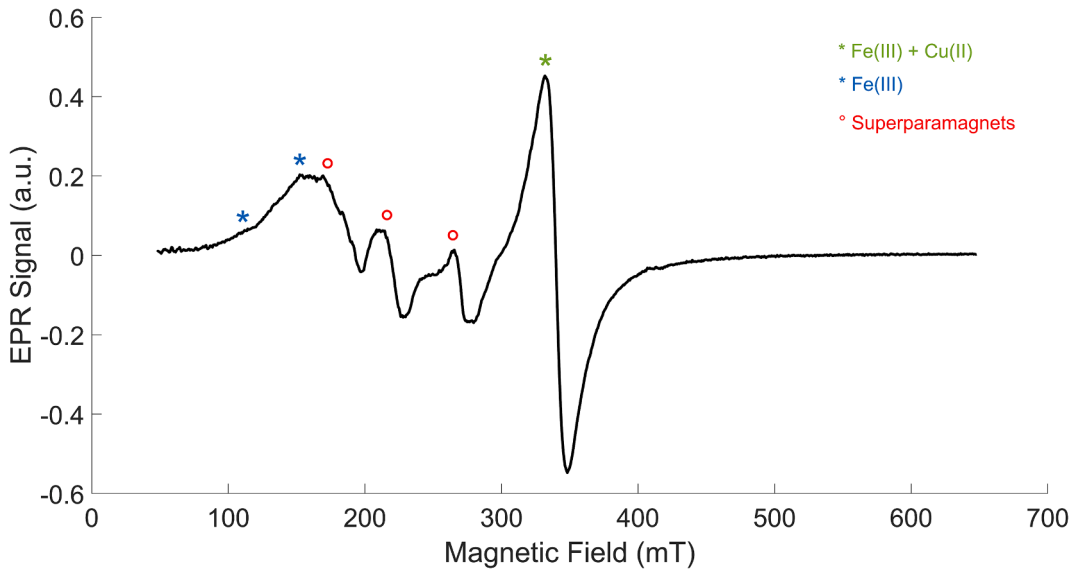

Fig. 3. Raw azurite (AZ) CW-EPR spectrum at X-band collected at room temperature. The blue asterisks indicate the Fe(III) signals, while the red circles are related to superparamagnetic species signals (e.g., copper oxide, iron oxides, etc.). (For interpretation of the references to color in this figure legend, the reader is referred to the web version of this article.)

complexes emerge, but some residual signal related to the original raw malachite is still present. Although copper can easily bind proteins, the MLEW5 mixture seems unexpectedly similar to the raw pigment (Figure S7). In addition, new signals in the 180–300 mT spectral region emerge. These changes could suggest a different superparamagnetic arrangement due to the interaction with the binder (e.g. particles size). This is likely related to the solubility of the pigment in the different binders.

The MLn5 mixtures were studied by CW-EPR at 150 K to resolve better the Cu(II)-binder signals (Fig. 4a), quenching the superparamagnetic signals thanks to broadening and shifting of the spectral features. Due to the paramagnetic nature of the "copper soaps", the signal at 330 mT becomes more intense at lower temperature and it is possible to simulate it obtaining the main magnetic quantities (i.e., g-tensor and hyperfine coupling tensor).

The MLAG5, MLC5, MLY5 and MLEY5 spectra were simulated (Fig. 4b), and the parameters are collected in Table 1. Three species were necessary to get a suitable simulation. By plotting the hyperfine component A_{zz} vs. the g-tensor component g_{zz} in the diagrams of Peisach and Blumberg [23], it is possible to assign roughly the atoms in the first coordination sphere of the copper nuclei. The g and A parameters of MLAG5 are in the range for a copper atom with a four-oxygen (4O) coordination sphere (g_{zz} roughly between 2.27 and 2.43), as expected from a polysaccharide-based binder: specifically, the dominant species 2, with $g_{zz} = 2.35$ and $A_{zz} = 470$ MHz, matches well with a neutral species. A similar consideration holds for the species 3, whereas the species 1 corresponds likely to a negatively charged complex (higher A_{zz} value and lower g_{zz} value). On the other hand, the parameters for the species 1 and 2 in the MLY5 and MLEY5 samples are indicative of a first-coordination sphere with at least one nitrogen atom (whose g_{zz} values are less than 2.7, ruling out a 4O coordination), suggesting that the proteins can extract copper atoms from the pigment. The species 3 in MLY5 and MLEY5 has a g-value (2.29) which could fit both a 4O complex, with a −2 negative charge, or a neutral complex with configuration 1N3O or 2N2O. A 1N3O or 2N2O configuration is more likely, due to the hydrophobic environment in the yolk binder, making less favorable the presence of a charges. The species 1 and 2 of MLEY5 and MLY5 match well neutral complexes with 2N2O configuration. It is worth noting that the experimental EPR spectra of MLY5 and MLEY5 are substantially equal, resulting in a simulation with three species with the same magnetic parameters. Considering that the MLEW5 sample does not show clearly the presence of copper complexes similar to those obtained with the other two egg-based mixtures, this suggests that the protein in the fatty moiety of the egg (yolk) are more suitable to form complexes with Cu(II) cations for the pigment malachite. As aforementioned, this could be related to the different solubility of the malachite in the two different matrices. It is interesting to note that for MLC5, at 150 K, a specific binding for Cu(II) is obtained, with at least three main species, according to the simulation. Plotting the parameters of MLC5 in the Peisach-Blumberg diagrams, one can infer that the copper has more likely a 1N3O coordination, with the species 1 negatively charged, the species 2 neutral, and the species 3 neutral or positively charged. The collagen

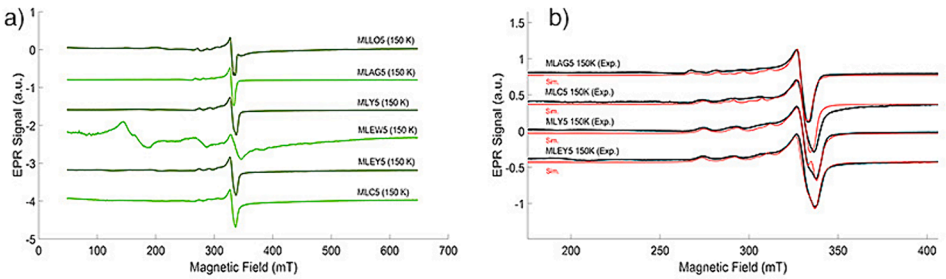

Fig. 4. a) cw-epr spectra at x-band of ml-binder mixtures, with a 5 % pigment, at 150 K and b) CW-EPR spectra (black line) at X-band of ML-binder mixtures with a 5 % pigment, acquired at 150 K, and overlapped simulations (red line) (LO = linseed oil, AG = Arabic gum, Y = yolk, EW = egg white, EY = egg white and yolk, and C = collagen). (For interpretation of the references to color in this figure legend, the reader is referred to the web version of this article.)

Table 1
Simulation parameters of MLn5 spectra at X-band collected at 150 K. The "weight" parameter is an absolute value that takes into account the amount of the single species. The parameters g_{xx}, g_{yy} and g_{zz} are the g-tensor main components. The parameters A_{xx}, A_{yy} and A_{zz} are the hyperfine tensor main components. In the last column are reported the suggested first coordination spheres based on Peisach-Blumberg diagram assignation (N = nitrogen atom, and O = oxygen atom).

Sample	Species	g_{xx}	g_{yy}	g_{zz}	A_{xx} (MHz)	A_{yy} (MHz)	A_{zz} (MHz)	Weight	Suggested first coordination sphere
MLY5 150 K	1	2.068	2.05	2.25	10	10	560	0.6	1N3O – 2N2O
MLY5 150 K	2	2.07	2.05	2.27	10	10	530	0.1	1N3O – 2N2O
MLY5 150 K	3	2.07	2.05	2.29	10	10	510	0.3	1N3O – 2N2O
MLEY5 150 K	1	2.068	2.05	2.25	10	10	560	0.6	1N3O – 2N2O
MLEY5 150 K	2	2.07	2.05	2.27	10	10	530	0.1	1N3O – 2N2O
MLEY5 150 K	3	2.07	2.05	2.29	10	10	510	0.3	1N3O – 2N2O
MLC5 150 K	1	2.062	2.047	2.275	10	10	490	0.5	1N3O
MLC5 150 K	2	2.062	2.047	2. 303	10	10	460	0.4	1N3O
MLC5 150 K	3	2.062	2.047	2.32	10	10	440	0.1	1N3O
MLAG5 150 K	1	2.075	2.06	2.288	10	10	540	0.25	4O
MLAG5 150 K	2	2.075	2.06	2.35	10	10	470	0.55	4O
MLAG5 150 K	3	2.075	2.06	2.37	10	10	460	0.2	4O

contains water, and it is easier to have free charges in this polar matrix, while the yolk and the egg white-yolk mixtures have a more apolar environment. It is not unexpected that protein binders can form easily copper complexes, extracting copper ions from the pigment, due to the ability of nitrogen atoms to bind Cu(II) ions. It is interesting to note that also non-protein binders, like linseed oil and Arabic gum, can do it. For this latter binder, considering the neutral complexes, it is likely that two oxygen atoms comes either from –OH groups of mono-saccharide units (e.g. arabinose, galactose, rhamnose), and the other two could be related to water molecules, or two bi-dentate glucuronic acid units (COO– groups) [2]. On the contrary, the negative and the positive species arise by the coordination of several different oxygen-donors. This suggest that the copper atoms are embedded in the polysaccharide matrix in several, different ways, and this probably could lead to a faster curing of the pictorial layer.

4.3. CW-EPR: AZnr pictorial mixtures

Similarly, the azurite pigment shows some spectral differences when combined with the binders. The AZn75 mixtures show different features depending on the binder (Figure S8). In particular, the AZY75 and AZC75 show the appearance of a quite intense feature at 150 mT related to a Fe(III) ion in a rhombic site. In general, the spectra are completely different with all the binders compared to the azurite one, suggesting that the interaction between the pigment and the binder induced some modifications in the structure of the former (e.g., complexes formation, solubilization and re-precipitation, changing in the pigment particles size, etc.). However, it is very difficult following all the changes by CW-EPR spectroscopy. In order to highlight the emerging of copper complexes, the AZn5 mixtures were prepared and analyzed (Figure S9). In all the samples, clearly emerges the presence of Cu(II)-binder complexes, as observed for malachite. However, in some cases the signal is likely superimposed to the one of Fe(III) in octahedral site. The linewidth suggest the presence of several Fe(III) complexes, indicating once again that the binder can modify the coordination of these ions, that are present in the pigment as natural impurities. In order to enhance the intensity of the paramagnetic signal of copper complexes, the CW-EPR spectra of the samples were collected at 150 K (Fig. 5a). What emerges is that the features not related to the copper complexes are quenched, and the typical quartet signal emerges in all the samples. However, the majority of the spectra shows strong distortion due to residual signals of Fe^{3+} species. It was possible to simulate the spectrum in just one case: the AZY5 sample (Fig. 5b). Looking at the simulation parameters (Table 2) and comparing them with those obtained for the malachite samples, it emerges that are equal to those of MLY5 sample (and therefore, similar considerations hold). This suggest that in the two cases the proteins of the yolk coordinate the copper atoms in the same way. However, the line broadening prevents a more precise assignation.

5. Conclusion

This study highlights the effectiveness of the CW-EPR spectroscopy in characterizing the magnetic nature of the pigments (natural malachite and natural azurite), and identifying the interaction products between the pigments and the binders, which are challenging to be assessed using other spectroscopic methods. These products, commonly called as "metal soaps", are suspected to be related to the degradation of many historical artifacts. Herein, we have demonstrated that the nature of these copper complexes can significantly vary depending on the organic binder used and that different binders exhibit variable affinities towards copper ions. Therefore, the EPR technique can serve as both an identification tool for use in artifacts and as a "sensor" for monitoring the formation of detrimental metal soaps (with paramagnetic transition metals). Finally, the findings presented in this study pave the way for the application of advanced EPR experiments such as ESEEM (Electron Spin Echo Envelope Modulation), ENDOR (Electron Nuclear Double Resonance), and others, which could offer a deep insight into the properties of the copper complexes.

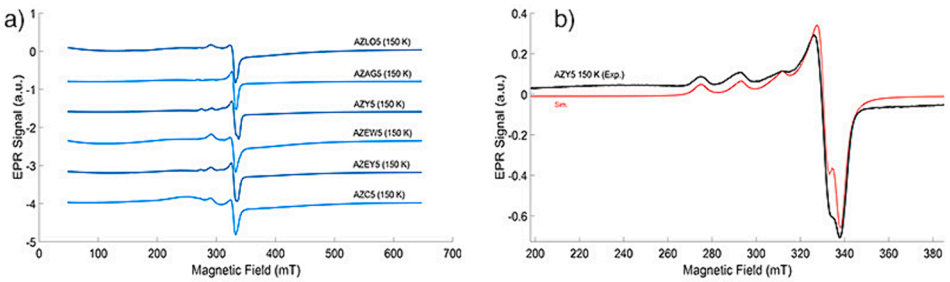

Fig. 5. a) cw-epr spectra at x-band of az-binder mixtures, with a 5 % pigment, at 150 K, and b) CW-EPR spectrum at X-band of AZY5 sample at 150 K (black line) and the corresponding simulated spectrum (red line) (LO = linseed oil, AG = Arabic gum, Y = yolk, EW = egg white, EY = egg white and yolk, and C = collagen). (For interpretation of the references to color in this figure legend, the reader is referred to the web version of this article.)

Table 2
Simulation parameters of AZY5 spectrum at X-band collected at 150 K. The "weight" parameter is an absolute value that takes into account the amount of the single species. The parameters g_{xx}, g_{yy} and g_{zz} are the g-tensor main components. The parameters A_{xx}, A_{yy} and A_{zz} are the hyperfine tensor main components. In the last column are reported the suggested first coordination spheres based on Peisach-Blumberg diagram assignation (N = nitrogen atom, and O = oxygen atom).

Sample	Species	g_{xx}	g_{yy}	g_{zz}	A_{xx} (MHz)	A_{yy} (MHz)	A_{zz} (MHz)	Weight	Suggested first coordination sphere
AZY5 150 K	1	2.068	2.05	2.25	10	10	560	0.6	1N3O – 2N2O
AZY5 150 K	2	2.068	2.05	2.27	10	10	530	0.2	1N3O – 2N2O
AZY5 150 K	3	2.068	2.05	2.29	10	10	510	0.2	1N3O – 2N2O

Author contribution

The manuscript was written through contributions of all authors. All authors have given approval to the final version of the manuscript. R.P: performed the EPR spectroscopies experiments and the data processing. R.P. and A.Z. discussed the results. The paper was written by R.P., and reread by the other author.

Funding research.

This work was funded under the National Recovery and Resilience Plan (NRRP) and the NextGeneration EU Project (CUP. C96E22000460007; Grant code: 38–413-19-DOT1319897-8969). The authors acknowledge the Fondazione Zegna for its economical contribution under the Ermenegildo Zegna Founder's Scholarship.

CRediT authorship contribution statement

Riccardo Punis: Writing – review & editing, Writing – original draft, Methodology, Investigation, Funding acquisition, Formal analysis, Data curation. **Alfonso Zoleo:** Writing – review & editing, Validation, Supervision, Conceptualization.

Declaration of competing interest

The authors declare that they have no known competing financial interests or personal relationships that could have appeared to influence the work reported in this paper.

Data availability

The authors are unable or have chosen not to specify which data has been used.

Acknowledgements

We are grateful to Emanuela Zangirolami and Sabrina Mattiolo for her technical support.

Appendix A. Supplementary data

Supplementary data to this article can be found online at https://doi.org/10.1016/j.microc.2024.110303.

References

[1] Cennino, C.. XIV-XV century. *The Book of the Art of Cennino Cennini: A Contemporary Practical Treatise on Quattrocento Painting*. Translated by J.C. Herringham. London: George Allen, Ruskin House.
[2] J.S. Mills, R. White, *The organic chemistry of museum objects, 2nd edition*, arts and archaeology, Butterworth-Heinmann Ltd., Oxford, 1994.
[3] R.G. Burns (Ed.), Mineralogical Applications of Crystal Field Theory, 2nd edition, Cambridge University Press, 1993.
[4] R.J. Gettens, Identification of the materials in paintings, Stud. Conserv. 11 (2) (1966) 52–53.
[5] K. Hills-Kimball, I. Lovelace, I. Peng, J. Wang, H.F. Garces, M. Rios, O. Chen, L.-Q. Wang, New insights to the interactions between amorphous georgite pigment and linseed oil binder that Lead to a drastic color change, Inorg. Chim. Acta 529 (2022) 120661.
[6] R. Punis, A. Zoleo, Copper complexes in verdigris painting mixtures: an electron paramagnetic resonance characterization, Restaurator, International Journal for the Preservation of Library and Archival Material, 2023.
[7] Punis, R.; Veronese, M.; Meneghetti, M.; Zoleo, A. Copper Soaps Formation in Verdigris–Linseed Oil Painting Mixtures: A Multispectroscopic Characterization. *Inorg. Chem.* 2024, acs.inorgchem.3c03794.
[8] Z. Zoleo, L. Nodari, M. Rampazzo, F. Piccinelli, U. Russo, C. Federici, M. Brustolon, Characterization of pigment and binder in badly conserved illuminations of a 15th-century manuscript, Archaeometry 56 (3) (2014) 496–512.
[9] M. Alter, L. Binet, N. Touati, N. Lubin-Germain, A. Le Hô, F. Mirambet, D. Gourier, Photochemical origin of the darkening of copper acetate and resinate pigments in historical paintings, Inorg. Chem. 58 (19) (2019) 13115–13128.
[10] Abragam, A.; Bleaney, B. Spin-Spin Interaction. In Electron Paramagnetic Resonance of Transition Ions, Reprint ed.; The International Series of Monographs on Physics; Oxford University Press, 2012.
[11] M. Brustolon, E. Giamello, Electron paramagnetic resonance: a practitioner's toolkit, John Wiley and Sons Inc, Publication, Hoboken, 2008.
[12] M. Romanelli, A. Buccianti, F. Di Benedetto, L. Bellucci, S. Cemicky, An innovative electron paramagnetic resonance and statistical analysis approach to investigate the geographical origin of multi-layered samples from a renaissance painting, Microchem. J. 177 (2022) 107219.
[13] M. Agrachev, L. Nodari, S. Gualtieri, A. Zoleo, Probing firing-induced changes in non-carbonate clay through 55Mn EPR techniques, Appl. Clay Sci. 132–133 (2016) 313–319.
[14] A. Zoleo, D. Confortin, N. Dal Mina, M. Brustolon, The role of metal ions in the study of ancient paper by electron paramagnetic resonance, App. Magn. Reson. 39 (3) (2010) 215–223.
[15] C. Santoro, K. Zarkout, A.S. Le Hô, F. Mirambet, D. Gourier, L. Binet, S. Pagès-Camagna, S. Reguer, S. Mirabaud, Y. Le Du, P. Griesmar, N. Lubin-Germain, M. Menu, New highlights on degradation process of verdigris from easel paintings, Appl. Phys. A 114 (2014) 637–645.
[16] S. Stoll, A. Schweiger, EasySpin, a comprehensive software package for spectral simulation and analysis in EPR, J. Magn. Reson. 178 (1) (2006) 42–55.
[17] A. Zoleo, M. Brustolon, A. Barbon, A. Silvestri, G. Molin, S. Tonietto, Fe(III) and Mn (II) EPR quantitation in glass fragments from the palaeo-christian mosaic of st. prosdocimus (padova, NE Italy): archaeometric and colour correlations, J. Cult. Herit. 16 (3) (2015) 322–328.
[18] Z. Tomkowicz, P. Fleischhauer, W. Hasse, M. Baran, R. Szymczak, A.J. Zaleski, Magnetic properties of two trimeric CU(II) complexes with ferromagnetic intratrimer interaction, J. Magn. Magn. Mater. 127 (1993).
[19] A.-L. Barra, P. Debrunner, D. Gatteschi, C.E. Schulz, R. Sessoli, Superparamagnetic-like behavior in an octanuclear iron cluster, Europhys. Lett. 35 (2) (1996) 133–138.
[20] S. Lebernegg, A.A. Tsirlin, O. Janson, H. Rosner, Spin gap in malachite cu 2 (OH) 2 CO 3 and its evolution under pressure, Phys. Rev. B 88 (22) (2013) 224406.
[21] H. Jeschke, I. Opahle, H. Kandpal, R. Valentí, H. Das, T. Saha-Dasgupta, O. Janson, H. Rosner, A. Brühl, B. Wolf, M. Lang, J. Richter, S. Hu, X. Wang, R. Peters, T. Pruschke, A. Honecker, Multistep approach to microscopic models for frustrated quantum magnets: the case of the natural mineral azurite, Phys. Rev. Lett. 106 (21) (2011) 217201.
[22] V. Marghussian, Properties of Nano-glass ceramics, William Andrew Publishing, Oxford, Nano-Glass Ceramics, 2015, pp. 181–223.
[23] J. Peisach, W.E. Blumberg, Structural implications derived from the analysis of electron paramagnetic resonance spectra of natural and artificial copper proteins, Arch. Biochem. Biophys. 165 (2) (1974) 691–708.